

Tip-enhanced Raman scattering from bridged nanocones

Satish Rao,¹ Mikko J. Huttunen,² Juha M. Kontio,³ Jouni Makitalo,²
Milla-Riina Viljanen,³ Janne Simonen,³ Martti Kauranen,² and
Dmitri Petrov,^{1,4,*}

¹*ICFO - Institut de Ciències Fotòniques, Mediterranean Technology Park, 08860 Castelldefels (Barcelona), Spain*

²*Department of Physics, Tampere University of Technology, FI-33101 Tampere, Finland*

³*Optoelectronics Research Centre, Tampere University of Technology, FI-33101 Tampere, Finland*

⁴*ICREA - Institució Catalana de Recerca i Estudis Avançats, 08010 Barcelona, Spain*

*Dmitri.Petrov@icfo.es

Abstract: We present two silver nanocones separated by 450 nm, well beyond the typical gap spacing of coupled nanoantennas, and connected by a metal bridge to facilitate plasmonic coupling between them. The tip-enhanced Raman scattering from crystal violet molecules is found to be almost an order of magnitude higher from the bridged cones than from individual cones. This result is supported by local-field calculations of the two types of structures. The bridged nanocones are easily fabricated by a nanoimprint-based process, thus offering a faster and simpler approach compared to other fabrication techniques.

© 2010 Optical Society of America

OCIS codes: (240.6695) Surface-enhanced Raman scattering; (300.6280) Spectroscopy, fluorescence and luminescence; (240.6680) Surface plasmons; (240.3990) Micro-optical devices.

References and links

1. M. Brongersma and V. Shalaev, "The case for plasmonics," *Science* **328**, 440–441 (2010).
2. X. Hoa, A. Kirk, and M. Tabrizian, "Towards integrated and sensitive surface plasmon resonance biosensors: a review of recent progress," *Biosens. Bioelectron.* **23**, 151–160 (2007).
3. D. Ward, N. Grady, C. Levin, N. Halas, Y. Wu, P. Nordlander, and D. Natelson, "Electromigrated nanoscale gaps for surface-enhanced Raman spectroscopy," *Nano Lett.* **7**, 1396–1400 (2007).
4. E. Bailo and V. Deckert, "Tip-enhanced Raman scattering," *Chem. Soc. Rev.* **37**, 921–930 (2008).
5. T. Yano, P. Verma, Y. Saito, T. Ichimura, and S. Kawata, "Pressure-assisted tip-enhanced Raman imaging at a resolution of a few nanometres," *Nat. Photonics* **3**, 473–477 (2009).
6. F. Angelis, G. Das, P. Candeloro, P. Maddalena, M. Galli, A. Bek, M. Lazzarino, I. Maksymov, C. Liberale, L. Andreani, and E. Fabrizio, "Nanoscale chemical mapping using three-dimensional adiabatic compression of surface plasmon polaritons," *Nat. Nanotechnol.* **5**, 67–72 (2010).
7. C. Hsu, S. Connor, M. Tang, and Y. Cui, "Wafer-scale silicon nanopillars and nanocones by Langmuir-Blodgett assembly and etching," *Appl. Phys. Lett.* **93**, 133109 (2008).
8. J. Kontio, J. Simonen, J. Tommila, and M. Pessa, "Arrays of metallic nanocones fabricated by uv-nanoimprint lithography," *Microelectron. Eng.* **87**, 1711–1715 (2010).
9. C. Rockstuhl, F. Lederer, C. Etrich, T. Zentgraf, J. Kuhl, and H. Giessen, "On the reinterpretation of resonances in split-ring-resonators at normal incidence," *Opt. Express* **14**, 8827–8836 (2006).
10. T. Corrigan, P. Kolb, A. Sushkov, H. Drew, D. Schmadel, and R. Phaneuf, "Optical plasmonic resonances in split-ring resonator structures: an improved lc model," *Opt. Express* **16**, 19850–19864 (2008).
11. I. Mikhailyuk and A. Razzhivin, "Background subtraction in experimental data arrays illustrated by the example of raman spectra and fluorescent gel electrophoresis patterns," *Instrum. Exp. Tech.* **46**, 765–769 (2003).

12. A. Kudelski, "Raman studies of rhodamine 6G and crystal violet sub-monolayers on electrochemically roughened silver substrates: do dye molecules adsorb preferentially on highly SERS-active sites?" *Chem. Phys. Lett.* **414**, 271–275 (2005).
 13. X. Jiao, J. Goeckeritz, S. Blair, and M. Oldham, "Localization of near-field resonances in bowtie antennae: influence of adhesion layers," *Plasmonics* **4**, 37-50 (2009).
 14. R. Harrington, *Field computation by moment methods* (Wiley-IEEE Press, 1993).
 15. C. Geuzaine and J.-F. Remacle, "Gmsh: a three-dimensional finite element mesh generator with built-in pre- and post-processing facilities," *Int. J. Numer. Methods Eng.* **79**, 1309–1331 (2009).
 16. L. Novotny, R. X. Bian, and X. S. Xie, "Theory of nanometric optical tweezers," *Phys. Rev. Lett.* **79**, 645–648 (1997).
 17. X. Ling, L. Xie, Y. Fang, H. Xu, H. Zhang, J. Kong, M. Dresselhaus, J. Zhang, and Z. Liu, "Can graphene be used as a substrate for Raman enhancement?" *Nano Lett.* **10**, 553–561 (2010).
 18. H. Frey, S. Witt, K. Felderer, and R. Guckenberger, "High-resolution imaging of single fluorescent molecules with the optical near-field of a metal tip," *Phys. Rev. Lett.* **93**, 200801 (2004).
-

1. Introduction

The plasmonics field has progressed in producing ordered systems that enhance the optical fields applied onto, emitted, and scattered by metal nanostructures [1]. Such structures have the potential to be integrated in to numerous lab-on-a-chip applications such as high throughput analyte detection [2]. The work to date has included various forms of nanoantennas that utilize nanosized gaps between metal structures [3] and metal tips whose apex sizes lie in the range of tens of nanometers. The latter have been studied extensively for tip-enhanced Raman scattering (TERS), a specialized form of surface-enhanced Raman scattering (SERS), where strong local fields at the tip enhance the Raman signal at spatial resolutions on the order of the tip apex size [4]. An advantage of such tip structures is that they offer field enhancement along the third dimension, away from the planar surface, which could be useful for certain lab-on-a-chip and optical trapping applications, for example. Additionally, their position can be accurately controlled as a movable probe when attached to an atomic force microscope (AFM) [5].

The development of high-quality tips has depended on the choice of metal and patterning processes. For example, focused ion-beam milling (FIB) and electron-beam lithography (EBL) have produced nanocones, however, the processes are complicated, slow, and expensive [6]. Various forms of self-assembly and etching techniques [7] have also been employed although they fail to achieve similar tip sharpness when compared to FIB and EBL techniques. We have recently demonstrated a fast and robust method for constructing reproducible nanocone structures by utilizing UV-nanoimprint lithography (UV-NIL) combined with electron-beam evaporation [8].

With the nanocones in hand, previous efforts have attempted, with success, to further improve the field enhancing capability of these structures. For example, single cones made from silicon based materials were used with a deposited thin layer of metal to facilitate the plasmon effects [5]. Another successful method attached a single nanocone, constructed by FIB, to a photonic crystal cavity [6]. The system was constructed to couple the excitation light to the surface plasmons in the nanocone via surface plasmon polaritons, which led to the observation of Raman signal from a single chemical monolayer. Although signal enhancements have been achieved, the processes to construct such devices require multiple steps which can prove to be costly when a chip of structures is needed.

In this paper, we demonstrate a simple approach to prepare bridged nanocones with sharp tips that outperform single nanocones in terms of the achievable Raman signal enhancement. Two silver nanocones are connected by a silver bridge that overcomes the relatively large separation distance to achieve plasmon coupling between the two cones. The structure is intended to mimic the planar "U-shaped" split-ring-resonator (SRR) where plasmon coupling between two arms is facilitated through a base wire [9, 10]. Additionally, the sharp tips at the ends of the arms are

shown to be favorable for the field enhancement effects.

2. Methods

The method used for the single nanocone fabrication has been studied and reported previously [8]. Briefly, a master template having a lattice of both cylindrical holes (single nanocones) and connected hole pairs (bridged nanocones) was first prepared by EBL on a silicon wafer. The resulting nanopatterns were then copied to a transparent elastomer stamp made of poly(dimethylsiloxane) (PDMS). A glass substrate with thickness of $180\ \mu\text{m}$ was spin-coated with $800\ \text{nm}$ of polymethyl methacrylate (PMMA) and baked on a hotplate at 170°C for 2 min. Next, a $20\ \text{nm}$ thick Ge layer was deposited by electron-beam evaporation, serving as an etch-stop layer for improving the controllability of the etching steps and preventing intermixing of NIL and PMMA resist layers. A thin layer of NIL resist (Amonil from Amo GmbH) was then spun over the Ge layer followed by nanoimprinting with an EVG 620 mask aligner using the PDMS stamp. Following imprinting, reactive ion etching with a CHF_3/Ar based plasma chemistry was utilized to etch through the NIL resist and Ge layers. The PMMA layer was subsequently etched anisotropically with O_2 plasma, exposing the substrate. Note that the final structure does not contain Ge, which could significantly modify the plasmonic properties of the fabricated structure.

The conical shape of the nanocones was defined through metal deposition of a titanium adhesion layer ($20\ \text{nm}$) followed by evaporation of $1000\ \text{nm}$ of silver. In principle, any metal could be used, however, we choose silver due to its natural resonances around our excitation wavelength and the ability to obtain high aspect ratios with the material in order to realize concentrated fields far away from the glass surface. The conical shape is formed spontaneously when the holes in the mask shrink during the evaporation. The deposition was continued until the holes in the resist mask were completely filled with metal. The connecting bridge between the cones also forms spontaneously during the evaporation of the metal and contains small spikes due to grain formation. This grain formation is also a limiting factor of the overall quality of the nanocones. A lift-off process was performed in an acetone bath using ultrasonic agitation resulting in an array of metallic nanocones on the substrate. The quality of the structures was verified by field-emission scanning electron microscope (FE-SEM) (Fig. 1).

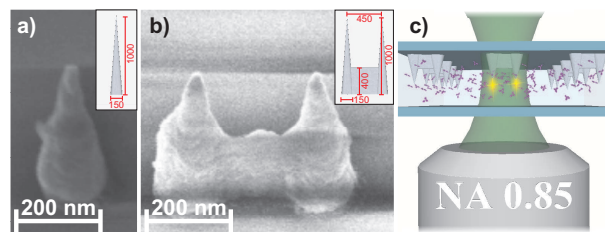


Fig. 1. FE-SEM images of the single (a) and bridged (b) nanocones structures with drawings depicting their dimensions included (insets). An illustration (c) of the orientation of the cones in the experimental setup is also given.

Each cone had a base diameter of $150\ \text{nm}$ and a height of approximately $1\ \mu\text{m}$ with a final tip radius of curvature of approximately $5\ \text{nm}$. The array period of the single cones was $1\ \mu\text{m}$. The bridged nanocone structures were made up of two cones separated by $450\ \text{nm}$ and connected with the metal bridge in an array of the same periodicity as the single cones. The bridge was $50\ \text{nm}$ wide and $330\ \text{nm}$ in height. We concluded this to be a safe geometry where the bridge is short enough such that the cone tips remain active while being large enough to avoid producing any additional local fields in the bridge itself. As a control, single nanocones with an array

period of 450 nm were also constructed and tested in order to mimic a pair of cones in the absence of a bridge.

For the experiments, the cones were immersed in an aqueous solution of crystal violet (CV) (10^{-6} M) by placing drops of the solution on top of the cones and then enclosing the system with a second coverslip. The construct was held by a custom made sample holder before being placed on a microscope stage. The excitation beam (532 nm at 9 mW) was incident normal to the glass surface with the cones inverted such that the beam passed through the tip before the base (Fig. 1c). Similar to the SRR, we expect maximum fields to be produced with an excitation polarization parallel to the bridge, and so, we keep the polarization fixed in this direction for all experiments. The emission from the cones was collected in the backscattered direction through the same objective ($60\times$ NA = 0.85) that passes the excitation beam. The backscattered light was passed to a spectroscopic confocal detection system. The acquisition time for all spectra was 1 s.

3. Raman emission enhancement by nanocone structures

A comparison of the emitted signals from the structures in the presence of CV molecules is given in Fig. 2. The Raman and fluorescence bands of the CV molecules are clearly observed

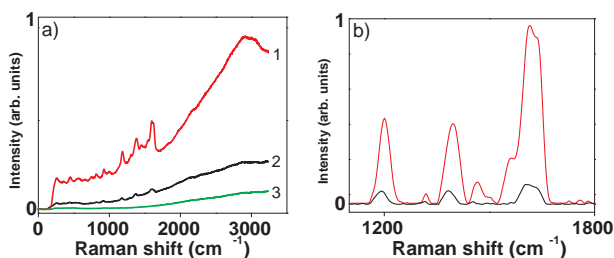


Fig. 2. (color online) a) The emission spectra for the bridged nanocones (1) and single nanocone (2) in the presence of CV. The background signal (3), obtained by measuring from a point in the solution away from the cones, is given. b) The resulting Raman bands after the CV fluorescence background has been removed demonstrating the TERS enhancement improvement of the bridged nanocones (red) compared to the single nanocone (black).

and at this dye concentration, no Raman signal and a low fluorescence signal above noise was observed at the same excitation power in the absence of nanocones. The broad emission peak at 2900 cm^{-1} (630 nm) is the main fluorescence band of CV and acts as background for the CV Raman spectrum. The fluorescence background is removed using an established method [11] in order to further distinguish the Raman bands (Fig. 2b). The three main peaks, at 1200 , 1400 , and 1615 cm^{-1} , agree with previous observations of the CV SERS spectrum [12].

The bridge clearly alters the optical properties of the system leading to a 4-fold increase in the fluorescence output from the single nanocone. The TERS enhancement is even higher: the three main CV peaks experience an average 8-fold Raman intensity increase relative to the single nanocone. Finally, the control structures, single nanocones at a period of 450 nm, produced spectra (data not shown) nearly identical to the single cone, thus further solidifying the positive effect of the bridge.

4. Local field analysis

The mechanisms for the differing enhancements of the Raman and fluorescence emission will be discussed later, however, both are a consequence of the local fields produced by the optically

excited structures. Thus, in order to facilitate the comparison, we conducted simulations to obtain the local electric field amplitude distributions for three structures: single cone, two cones separated by 450 nm, and the bridged nanocones structure. Due to the large structure height and similarity of the refractive indices of water and glass, the presence of the substrate and thin Ti adhesion layer were neglected. The absorption of Ti may, though, cause small decrease and shift of the resonances as estimated in [13]. We adopted the frequency domain method of moments (MOM) [14] where a focused beam was used as the input field. The surface mesh of the nanocone was generated with the free software Gmsh [15]. The input polarization of the beam was set to be linear and parallel to the plane of the cones and the focusing conditions matched those of the experiment. The focal field distribution was calculated using vector diffraction theory.

The results of the field calculations are presented in Fig. 3. The improved performance of

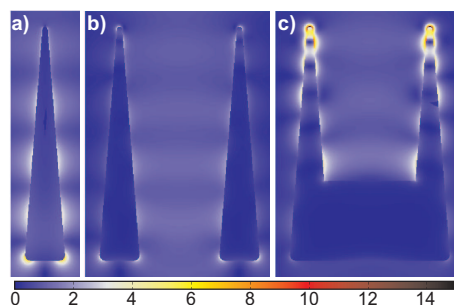


Fig. 3. Local field amplitude distribution simulations for three structures: single nanocone (a), two nanocones separated by 450 nm (b), and the bridged nanocones structure (c). The amplitudes were normalized to the maximum value of the focused beam without the structures. A 5-fold increase in field amplitude is observed at the tips of the bridged structure compared to single nanocones.

the bridged nanocones is immediately apparent where a 5-fold increase of the field amplitude at the tip is calculated compared to the single nanocone. As previously reported [16] there is no significant field enhancement near the tips with the single and two nanocone systems. This is due to the fact that a longitudinal field, i.e., a field with a component along the cone height axis, is needed to concentrate the local field into the tip [16]. The addition of the metal bridge breaks the symmetry of the single cone, facilitating the necessary coupling of electric field to the tips without the longitudinal field component. Only a transverse field component along the bridge is required, making the structure more feasible. Since the 532 nm excitation wavelength is away from the fundamental surface plasmonic resonances of the structure, the field enhancement is due to plasmonic resonances of higher-order [9]. The bridged nanocones structure mimics a metallic SRR that is U-shaped (for example, [9, 10]) where the bridge acts as the base wire and the cones as the two arms of the "U". The difference is that our version of the SRR is a three-dimensional structure with a large height that engineers the fields far away from the glass surface. Additionally, the cone shape forces higher localized fields at the tips without creating additional field concentrations at the bridge-cone interface edges, as is the case for the U-shaped SRR [10], thus optimizing the use of the input excitation while eliminating the additional non-radiative heating.

4.1. Discussion

The simulation results agree well with the experimental data. Generally for SERS and TERS, the intensity is proportional to the fourth power of the electric field because the field enhance-

ment occurs twice in this regime: the incident and scattered fields are equivalently amplified by the same plasmonic oscillations. Since the experimental TERS intensities are due to the total TERS signals from the molecules nearby and adsorbed to the cones, the volume integral of the quartic electric field amplitude over the focal volume should provide a qualitative agreement with the experiments. From the calculation, this value is 5 times greater in the bridged nanocones structures relative to the single cone, while an 8-fold increase is observed in the experiment where the average TERS intensity of the three main CV peaks is considered. The discrepancy can be related to the fact that the TERS intensity dependency on the fourth power of the electric field only considers the electromagnetic field enhancement. For many SERS systems, where molecules are also absorbed on to the metal surface, an additional chemical effect, where charges exchange directly between the molecule and the metal, should also be considered (for example, [17]). The secondary effect would add to the enhancement of the Raman signal and was not considered in our calculation. This would explain the existence of TERS signal from the single nanocone and the disparity between the measured and calculated relative enhancement factors between the bridged and single cones structures.

The mechanisms for the fluorescence enhancement are different because radiative and non-radiative processes are involved including some quenching due to the metal [18]. Thus, although an increase in the fluorescence enhancement is also observed from the bridged nanocones, connecting the local electric field intensity to a fluorescence enhancement factor is not clear, even at an estimation level, and is beyond the scope of this study.

Based on our current simulations and previous works, it is apparent that improvements can be made to the engineering of the bridge and in tailoring the light to be more specific, in regards to wavelength and polarization, to the structure. For example, the use of higher-order modes for excitation, such as radial polarization, could better couple the input electric field with the cones and further concentrate the fields into the tips. The physical parameters of the bridge must also play a role and could be tailored specifically to an excitation wavelength and the relationship of its dimensions to those of the cones should also be considered. Nevertheless, the results are clear: the bridged nanocones structure offers a decisive improvement in Raman enhancement compared to single cones. As mentioned previously here, there have been a number of attempts to improve the nanocone performance through additional complicated steps such as utilizing multi-layers of materials or photonic coupling to other structures. The distinct advantage here is the lack of additional processing steps in the fabrication method while leading to an improved performance. The structure remains suitable for lab-on-a-chip applications such as analyte detection or even biological studies such as spectroscopy of cells. This conclusion can also open doors to more complicated structures where multiple cones are utilized.

Acknowledgement

Spanish Ministry of Science and Innovation (MICINN/FIS2008-00114), Fundacion CELLEX Barcelona, the Academy of Finland (123109, 135084), and the Finnish Funding Agency for Technology and Innovation (40149/08). MJH acknowledges support from the Graduate School of Modern Optics and Photonics in Finland and the COST action MP0604. JMK acknowledges support from the graduate school of the Tampere University of Technology and Ulla Tuominen Foundation.